Short peptides are not reliable models of thermodynamic and kinetic properties of the N-terminal metal binding site in serum albumin

Magdalena Sokolowska[1], Artur Krezel[1], Marcin Dyba[1], Zbigniew Szewczuk[1] and Wojciech Bal[1,2]

[1]*Faculty of Chemistry, University of Wroclaw, Poland;* [2]*Institute of Biochemistry and Biophysics, Polish Academy of Sciences, Warsaw, Poland*

A comparative study of thermodynamic and kinetic aspects of Cu(II) and Ni(II) binding at the N-terminal binding site of human and bovine serum albumins (HSA and BSA, respectively) and short peptide analogues was performed using potentiometry and spectroscopic techniques. It was found that while qualitative aspects of interaction (spectra and structures of complexes, order of reactions) could be reproduced, the quantitative parameters (stability and rate constants) could not. The N-terminal site in HSA is much more similar to BSA than to short peptides reproducing the HSA sequence. A very strong influence of phosphate ions on the kinetics of Ni(II) interaction was found. This study demonstrates the limitations of short peptide modelling of Cu(II) and Ni(II) transport by albumins.

Keywords: serum albumin; copper(II); nickel(II); binding constants; rate constants.

Human serum albumin (HSA) is the most abundant protein of blood serum, at concentration of 0.63 mM ($\approx$ 4%) [1]. It is a versatile carrier protein, involved in the transport of hormones, vitamins, fatty acids, xenobiotics, drugs and metal ions, including physiological Ca^{2+}, Zn^{2+}, Co^{2+} and Cu^{2+}, as well as toxic Cd^{2+} and Ni^{2+} [1–3]. This variety of functions is made possible by the presence of many binding sites on the surface of the HSA molecule, including hydrophobic pockets of various sizes and shapes and coordination domains equipped with sets of donor groups appropriate for particular metals. Among the latter, the N-terminal binding site for Cu^{2+} and Ni^{2+} ions has been characterized particularly well. It is composed of the first three amino-acid residues of the HSA sequence, Asp-Ala-His, and the resulting square-planar complex exhibits a unique coordination mode with deprotonated amide

nitrogens of Ala and His residues, in addition to the N-terminal amine and the His imidazole donor (the so-called 4N complex, see Fig. 1) [4–7]. Structural studies on various peptide analogues in the solid state [8–10] and in solution [11,12], as well as numerous spectroscopic works confirmed that such coordination style is a common feature of peptides having N-terminal sequences of the X-Y-His type (reviewed in [13]). As such, it is shared by many mammalian albumins, which differ from HSA at positions 1 and/or 2, but not 3 (e.g. bovine serum albumin, BSA, contains the sequence Asp-Thr-His) [14–17]. In albumins from several species, including dog (DSA) and pig (PSA), the His3 residue is replaced by Tyr. This, and any other mutation removing His from position 3, results in a lack of affinity and specificity for Cu(II) and Ni(II) binding at the N-terminus [7,16,18,19].

Recently, we have reported the existence of the second specific binding site for Cu(II) in HSA and BSA, which also shares spectroscopic similarities with a PSA site [20]. We named it 'multimetal binding site', because it can bind Ni(II), Zn(II) and Cd(II) with similar affinities. Based on information from [113]Cd NMR studies [21] and HSA crystallography [2,22], this site was located at the interface of domains I and II of HSA and BSA, where His67 and His247 are present on the protein surface, adjacent to each other. This site is at a distance of ≈ 16.5 Å from Ser5, the first N-terminal residue seen in electron density maps. For simplicity, the N-terminal site will be labelled 'site I' and the multimetal binding site 'site II' throughout the text. The analysis of binding constants obtained from CD-monitored metal ion titrations indicated that site II may have physiological relevance for Ni(II), Zn(II) and Cd(II). This finding is of particular interest for the yet unrecognized process of blood transport of toxic and carcinogenic nickel. It has been established that the Ni(II) complex at site I provides the antigenic moiety in nickel allergy [23,24], but little is known about the redistribution of nickel from blood
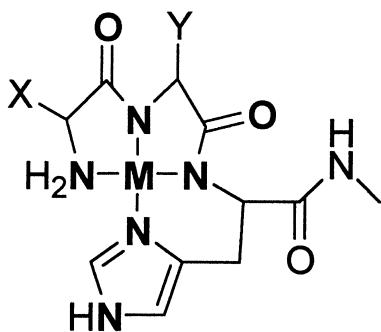
Fig. 1. Scheme of 4N coordination mode in XYH peptides, M is Cu(II) or Ni(II).

to organs in which it can exert procarcinogenic lesions [25]. In order to approach the issue of Cu(II) and Ni(II) exchange by albumin, we characterized the binding parameters and performed parallel kinetic studies using HSA and BSA and three simple analogues of the N-terminal binding site. These were: Asp-Ala-His-NH$_2$ (DAHam) and Asp-Ala-His-Lys-NH$_2$ (DAHKam), which represent the native HSA sequence and Val-Ile-His-Asn (VIHN), the N-terminal peptide of another blood serum protein, des-angiotensinogen [11]. The structure of the Ni(II) complex of the latter contains a specific steric shielding, resulting in a particularly slow kinetics of Ni(II) dissociation. Somewhat surprisingly, we found that, despite the identical mode of coordination, important thermodynamic and kinetic parameters of Cu(II) and Ni(II) interactions could not be reproduced quantitatively by short peptides. The present paper presents the results of our studies.

MATERIALS AND METHODS

Materials

NiCl$_2$ and CuCl$_2$ were purchased from Fluka. HNO$_3$, KNO$_3$, EDTA, dimethylglyoxime and ethanediol were obtained from Aldrich. Tris/HCl, mono- and disodium phosphates were purchased from Merck. Homogeneous, high purity defatted HSA and BSA [6] and Val-Ile-His-Asn (VIHN) peptide were obtained from Sigma. Peptide Asp-Ala-His-NH$_2$ (DAHam) was a gift of Henryk Kozlowski, Faculty of Chemistry, University of Wroclaw. Stock solutions of NiCl$_2$ and CuCl$_2$ were standardized gravimetrically with dimethylglyoxime and complexometrically with EDTA, respectively. Concentrations of stock solutions of HSA and BSA were estimated spectrophotometrically at 279 nm [6] and by Cu(II) titrations (see below). Purities of both peptides were determined by potentiometric titrations to exceed 98%.

Peptide synthesis

The *N*-Fmoc-protected amino acids and Fmoc Rink amide MBHA resin were obtained from Nova Biochem (Calbiochem-Novabiochem AG, Läufelfingen, Switzerland). Benzotriazol-1-yloxytris(dimethylamino)phosphonium hexafluorophosphate (BOP) was purchased from Chem-Impex International (Chem-Impex International, Wood Dale, IL, USA). Trifluoroacetic acid, piperidine,

N,*N*-dimethylformamide (DMF) and *N*,*N*-diisopropylethylamine (DIPEA) were obtained from Riedel – de Haën (Riedel-de Haën GmbH, Seeize, Germany). Acetic anhydride (Ac$_2$O) was obtained from POCh (POCh S.A., Gliwice, Poland). Triisopropylsilane (TIS) was obtained from Lancaster (Lancaster Synthesis GmbH, Mühlheim am Main, Germany). Acetonitrile (HPLC grade) was obtained from J. T. Baker (J. T. Baker, Deventer, the Netherlands).

The peptide Asp-Ala-His-Lys-NH$_2$ was synthesized by Fmoc strategy on solid support [26–28] using Rink amide MBHA resin. Fmoc protection groups were removed by 25% piperidine in DMF. The N-Fmoc-amino acids (3 equiv.) were coupled by BOP (3 equiv.)/DIPEA (6 equiv.) procedure [27]. Coupling reaction was monitored by Kaiser (ninhydrin) test [27,28]. After coupling reactions acetic anhydride (3 equiv.)/DIPEA (6 equiv.) in DMF was used for capping of unreacted peptides chains. Cleavage was effected using a mixture of trifluoroacetic acid, H$_2$O, and TIS (v/v/v = 95/2.5/2.5) over a period of 2.5 h, followed by precipitation with diethyl ether [28]. The crude peptides were purified by preparative HPLC on the Alltech Econosil C18 10 U column (Alltech Associate, Inc., Deerfield, IL, USA), 5-μm particle size, 22 × 250 mm, eluting with 0.1% trifluoroacetic acid/water at a flow rate of 7 mL·min^{-1} with detection at 223 nm. Fractions collected across the main peak were assessed by HPLC analysis on Beckman Ultra-sphere ODS C18 column (Beckman Instruments, Inc., Fullerton, CA, USA), 5-μm particle size, 4.6 × 250 mm, eluting with 0.1% trifluoroacetic acid/water (solvent A) and 0.1% trifluoroacetic acid/80% acetonitrile/water (solvent B), using a gradient of 0% B to 100% B over 60 min at flow rate of 1 mL·min^{-1} and detection at 223 nm. Correct fractions were pooled and lyophilized to yield with solid of purity exceeding 99% as assessed by HPLC analysis of the final materials. Identity and purity of peptide was confirmed by mass spectrometry, utilizing a Finnigan MAT TSQ 700 (Finnigan MAT, San Jose, CA, USA) mass spectrometer equipped with a Finnigan electrospray ionization source. The m/z values found/calculated were 468.8/469.2 $(M + H)^+$ and 234.9/235.1 $(M + 2H)^{2+}$.

Potentiometry

Potentiometric titrations of VIHN, DAHKam, their complexes with Cu(II), as well as the DAHKam complex with Ni(II) in the presence of 0.1 M KNO$_3$ were performed at 25 °C over the pH range 3–11.5 (Molspin automatic titrator) with 0.1 M NaOH as titrant. Changes in pH were monitored with a combined glass-Ag/AgCl electrode (Russell) calibrated daily in hydrogen ions concentrations by HNO$_3$ titrations [29]. Sample volumes of 1.5 mL, with peptide concentrations of 1 mM and peptide molar excess over metal ion of 1.1–1.5 were used. The titration data were analysed using the SUPERQUAD program [30]. Standard deviations computed by SUPERQUAD refer to random errors only.

CD spectroscopy

The spectra were recorded at 25 °C on a Jasco J-715 spectropolarimeter, over the range of 240–800 nm, using 1 cm cuvettes. The spectra are expressed in terms of

$\Delta\varepsilon = \varepsilon_l - \varepsilon_r$, where ε_l and ε_r are molar absorption coefficients for left and right circularly polarized light, respectively. 1 mM peptide solutions and peptide molar excess over metal ion of 1.1 were used for pH titrations, while 0.5 mM peptide samples were used for kinetic measurements. Concentrations of albumin samples were 0.5 mM in protein, with varied metal ion amounts. The albumin samples for titrations and metal exchange kinetics measurements were kept at pH 7.4 (100 mM sodium phosphate buffer). The kinetics of metal binding to peptides and their exchange was studied in 100 mM Tris/HCl and in 100 mM phosphate buffers, both at pH 7.4.

UV–Vis spectroscopy

The kinetics of Ni(II) binding to DAH-am and substitution by Cu(II) in 100 mM phosphate buffer, pH 7.4 at 25 °C was studied on a Beckman DU-650 spectrophotometer, using monitor wavelength of 420 nm, and sampling interval of 5 s. For control purposes the spectra were also recorded in the range of 300–900 nm before and after reaction. In a separate experiment, a titration of DAHK-am with Ni(II) was performed, also monitored at 420 nm. All other experimental details were analogous to those used in CD spectroscopy.

EPR

The X-band EPR spectra of Cu(II) complexes of VIHN and DAHKam were obtained at 77 K (liquid nitrogen) on a Bruker ESP-300 spectrometer, using Cu(II) concentrations of 3 mM and Cu(II)-to-peptide ratios of 1 : 1. Ethanediol aqueous solution (30% v/v) was used as solvent for these measurements to ensure homogeneity of the frozen samples.

RESULTS

Complexation of Cu(II) and Ni(II) by model peptides and albumins

Among the systems under scrutiny in this work, the Ni(II) complexes of VIHN [11] and the DAHam complexes of Cu(II) and Ni(II) [31] were studied previously. Tables 1 and 2 thus present only the novel data: protonation constants for DAHKam and VIHN, and stability constants (log α values) of Cu(II)-VIHN, Cu-DAHKam and Ni-DAHKam systems. The parameters of CD and EPR spectra of all major complexes present at pH 7.4 are provided in Table 3.

Table 1. Protonation constants (log β values) for peptides at $I = 0.1$ M (KNO$_3$) and 25 °C. Standard deviations on the last digits are given in parentheses.

Species	DAHKam	VIHN
HL	10.52(2)	7.92(2)
H$_2$L	18.05(2)	14.48(2)
H$_3$L	24.32(2)	18.37(3)
H$_4$L	27.16(3)	

Table 2. Stability constants (log β values) of Ni(II) and Cu(II) complexes of peptides at $I = 0.1$ M (KNO$_3$) and 25 °C. Standard deviations on the last digits are given in parentheses.

Species	DAHKam-Ni	DAHKam-Cu	VIHN-Cu
MH$_2$L	21.48(3)	23.15(6)	
ML	10.04(3)	14.18(3)	
MH$_{-1}$L	4.84(1)	9.88(2)	
MH$_{-2}$L	−5.21(1)	−0.32(3)	−1.15(1)

Table 3. Parameters of CD and EPR spectra of 4N complexes of peptides and albumins at pH 7.4 and 25 °C.

Compound	CD Ni(II)		CD Cu(II)		EPR Cu(II)	
	λ (nm)	Δε (M^{-1}·cm^{-1})	λ (nm)	Δε (M^{-1}·cm^{-1})	A∥ (Gs)	g∥
VIHN	475	(−1.33)	552	(−0.72)	206	2.18
	407	(+0.65)	477	(+0.34)		
	271	(+1.35)	315	(+1.33)		
	261	(+1.56)	275	(−2.50)		
DAHam[a]	475	(−1.66)	561	(−0.95)	205	2.18
	409	(+1.05)	485	(+0.53)		
	263	(+1.32)	306	(+1.40)		
			270	(−2.79)		
DAHKam	475	(−1.90)	567	(−0.46)	200	2.19
	410	(+1.61)	489	(+0.48)		
	267	(+1.04)	308	(+0.72)		
			270	(−1.99)		
HSA[b]	476	(−1.38)	565	(−0.54)	207	2.18
	410	(+1.19)	486	(+0.49)		
			307	(+0.96)		
BSA[b]	479	(−1.79)	559	(−0.94)	200	2.18
	410	(+1.11)	480	(+0.40)		
			310	(+1.42)		

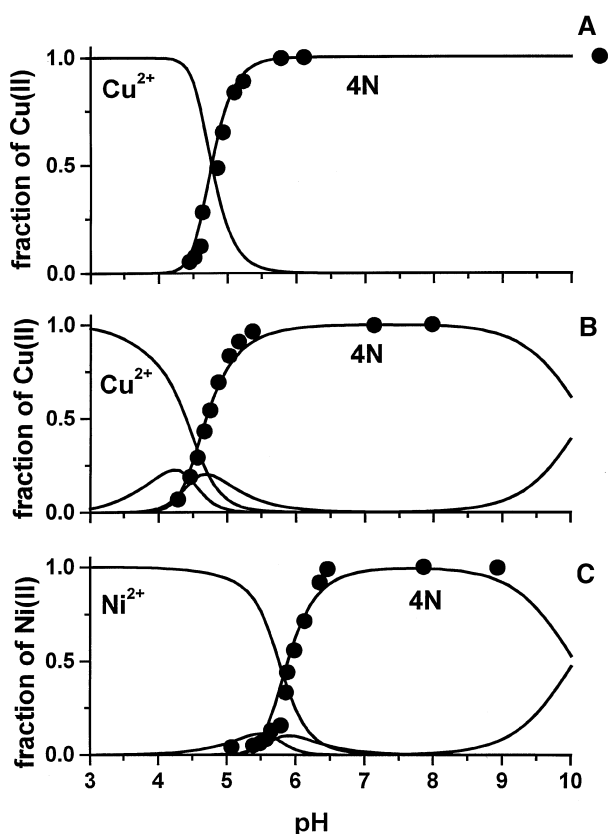[a] EPR data from [31]. [b] EPR data from [20].

Fig. 2. Speciation diagrams for VIHN-Cu(II) (A), DAHKam-Cu(II) (B) and DAHKam-Ni(II) (C), calculated for 0.5 mM concentrations of peptides and metal ions. The intensities of CD bands of 4N complexes (constructed by adding intensities at extremes of *d–d* bands and normalized to molar fractions) are overlapped as ● symbols.

The CD spectra for DAHam complexes at pH 7.4 were re-measured to assure full correspondence with kinetic experiments. Figure 2 presents potentiometric speciation diagrams for Cu(II)-VIHN, Cu-DAHKam and Ni-DAHKam systems, with relative CD intensities of the *d–d* bands of major 4N complexes overlaid (taken as $\Delta\varepsilon_{ext}$ of the higher energy component minus $\Delta\varepsilon_{ext}$ of the lower-energy component). The excellent agreement between these two independent measures of complex formation confirms the validity of the results.

CD spectra of albumins were found to be in good agreement with previous determinations, performed in the absence of buffers [20]. The application of 100 mM phosphate buffer at pH 7.4 (which conserves native conformations of the proteins) for albumin studies resulted in weak, but noticeable competition for Ni(II) binding at site I and Cu(II) binding at site II. No evidence of formation of ternary complexes was found. Also, no precipitation of metal phosphates or hydroxides occurred. Titration curves were obtained from the corresponding CD spectra, which allowed for calculations of appropriate conditional affinity constants. This is illustrated in Fig. 3 for Ni(II) binding at site I of HSA. Because of the slowness of Ni(II) binding at site I (see below), but not at site II, the equilibration of reaction at each point of Ni(II) titrations had to be assured by recording the spectra periodically. Quantitation of sites I
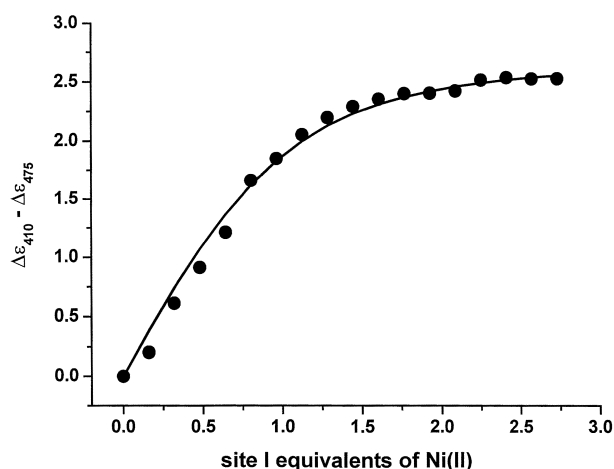

Fig. 3. Titration of site I in HSA with Ni(II) ions at pH 7.4 in 100 mM phosphate buffer. ●, experimental points constructed by adding intensities at extremes of *d–d* bands, 475 and 410 nm. Lines are fit to the conditional binding constant of Ni(II) at site I.

and II (and thus of albumin concentrations) could be obtained from Cu(II) titrations, as described in our previous paper [20]. In agreement with previous reports [20,32], the deficit of site I (25%) was found for HSA, but not for BSA. The binding constants for Ni(II) at site II were obtained from K_r, relative constants, describing Cu(II)/Ni(II) competition at site II. For BSA this constant was measured by the method described previously [20], based on titrating Cu(II) out of site II by Ni(II). This approach failed for HSA, which partially precipitated at higher excess of Ni(II). Therefore, this constant was calculated from kinetic experiments (see below). The $^2K_{Ni}$ value for BSA was obtained with site I occupied by Cu(II), and thus could be derived directly from fitting the titration curves. The values of $^2K_{Ni}$ constants were applied to calculate relative occupancies of sites I and II in the course of Ni(II) titrations. Finally, 'intrinsic' protein constants were calculated with the use of literature values of protonation and stability constants for phosphate complexes [33] These constants are presented in Table 4.

An analogous titration was performed for Ni(II) complexation by DAHKam, in 100 mM phosphate, pH 7.4, using absorption spectra. This titration yielded a linear increase of complex concentration up to the saturation, thus allowing for determination of ligand concentration, but not for stability constant calculations. This behaviour is indicative of a higher binding constant, making phosphate competition negligible.

The kinetics of Ni(II) binding to model peptides and albumins at pH 7.4 was also monitored by CD spectroscopy. In these experiments, the equimolar amounts of Ni(II) were added to buffered peptide or protein solutions in one portion, with subsequent periodical recording of the resulting CD spectra. The peptides were studied in both Tris and phosphate buffers, to find out whether the buffer components would affect the reaction rate. The reaction endpoint was not affected, because Cu(II) and Ni(II) binding capabilities of both buffers at pH 7.4 are almost identical to each other: log values of conditional affinity constants (^cK) of Tris complexes with Cu(II) and Ni(II),

Table 4. Binding constants (log values) for Cu(II) and Ni(II) complexes of albumins in 0.1 M phosphate buffer, pH 7.4, at 25 °C. Standard deviations on the last digit are given in parentheses.

Albumin	log $^1K_{Ni}$	log $^2K_{Ni}$[a]	log $^2K_{Cu}$	log K^τ	log($^1K_{Ni}/^2K_{Ni}$)
HSA	6.8(3)	4.9(3)	7.1(2)	2.18(5)	1.9(3)
BSA	6.69(8)	4.60(5)	6.20(3)	1.63(5)	2.09(8)

[a] Derived from K^τ determined experimentally using $^1K_{Ni}$.

Table 5. Values of apparent 1st order kinetic constants k_{obs} (s^{-1}) for Ni(II) binding and Ni(II) → Cu(II) exchange for model peptides and albumins in 100 mM Tris and phosphate buffers at 25 °C. Standard deviations on the last digits are given in parentheses.

Compound	k_{obs} (Ni + H$_n$L → NiH$_{-j}$L)		k_{obs} (NiH$_{-j}$L + Cu → CuH$_{-j}$L + Ni)	
	Tris	Phosphate	Tris	Phosphate
VIHN	$3.18(7) \times 10^{-4}$	$1.17(3) \times 10^{-3}$	$7(3) \times 10^{-7}$	$2.1(2) \times 10^{-6}$
DAHam	$1.72(5) \times 10^{-3}$	$3.2(2) \times 10^{-2}$	$1.17(3) \times 10^{-6}$	$1.90(3) \times 10^{-3}$
DAHKam	$5.8(1) \times 10^{-3}$	$2.1(1) \times 10^{-2}$	$9.2(8) \times 10^{-7}$	$3.0(1) \times 10^{-5}$
BSA		$2.56(7) \times 10^{-3}$		$7.5(3) \times 10^{-5}$
HSA		$2.7(1) \times 10^{-3}$		$1.57(8) \times 10^{-4}$
HSA → DAHKam				$3.2(2) \times 10^{-5}$

calculated from data in [34], are 3.4 and 1.9, respectively, vs. 3.1 and 2.0 for analogous phosphate complexes [33].

In all cases 1st order kinetic curves were seen. Table 5 presents the corresponding constants k_{obs}, obtained by least-square fitting of the curves generated using several reporter wavelengths, corresponding to spectral extrema. Examples of the spectra and kinetic plots are given for Ni(II) binding to DAHKam and HSA (Fig. 4).

Finally, the reaction of Ni(II) removal from site I by Cu(II) was studied for peptides [saturated at Ni(II)-to-peptide 1 : 1] and for albumins [in the presence of 1.5-fold molar excess of Ni(II) over site I, to assure its saturation]. The total amounts of Cu(II) and Ni(II) were matched in these measurements. In

a separate experiment, HSA saturated with Cu(II) at both sites was the source of Cu(II) competing for DAHKam saturated with Ni(II). The spectra and kinetic plots for HSA reaction are shown in Fig. 5.

DISCUSSION

Complex formation by model peptides

Potentiometric titrations and parallel CD and EPR spectroscopic measurements confirm that major complexes formed by peptides studied are typical 4N complexes of the structure presented in Fig. 1. For VIHN and DAHam
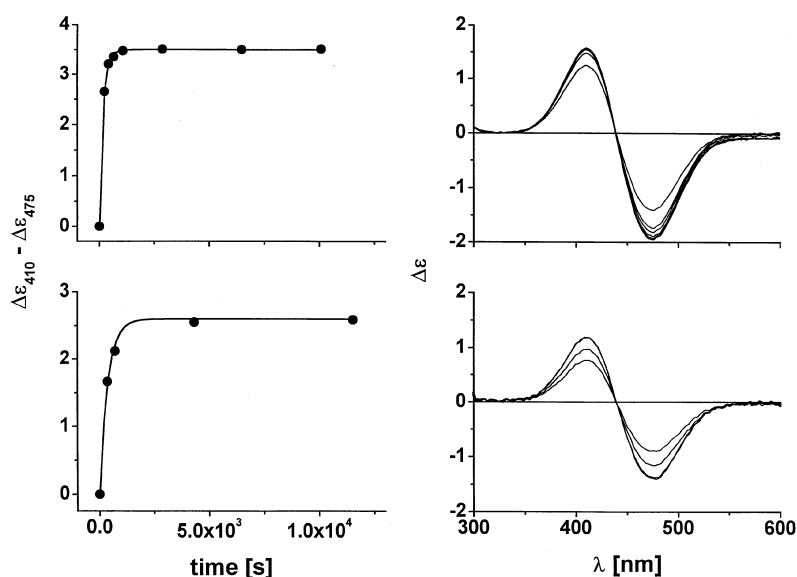

Fig. 4. Kinetics of Ni(II) binding to DAHKam and HSA at pH 7.4 in 100 mM phosphate buffer. Left panel, kinetic plots (●, experimental points constructed by adding intensities at extremes of *d–d* bands, 475 and 410 nm, lines are fits to 1st order kinetics). Right panel, the original CD spectra of Ni(II)-DAHKam (top) and Ni(II)-HSA (bottom).
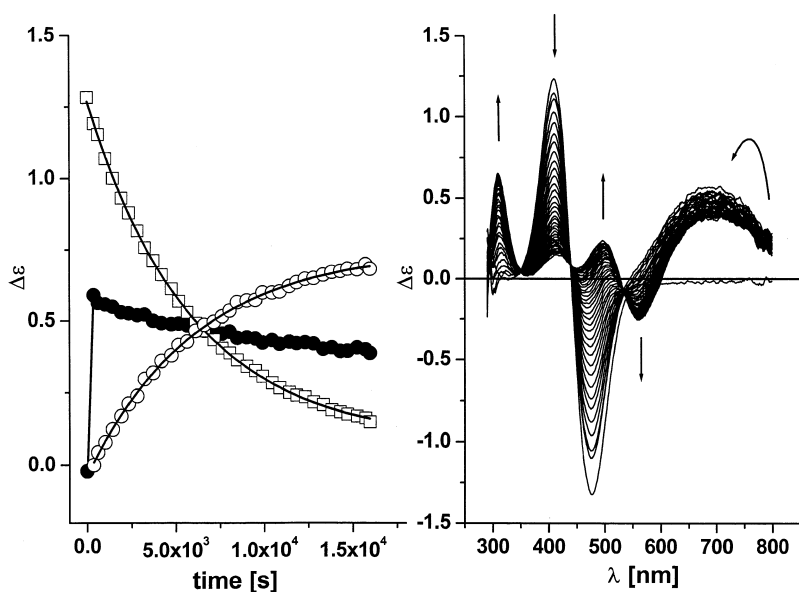
Fig. 5. Kinetics of Ni(II) substitution at site I of HSA by Cu(II) at pH 7.4 in 100 mM phosphate buffer. Left panel, kinetic plots of the loss of Ni(II) complex ($\square$, $\Delta\varepsilon$ at 410 nm), formation of Cu(II) complex ($\bigcirc$, $\Delta\varepsilon$ at 307 nm), and buffering of Cu(II) at site II ($\bullet$, $\Delta\varepsilon$ at 690 nm). Right panel, the original CD spectra. The arrows indicate directions of changes at particular wavelengths.

they are represented by the $MH_{-2}L$ formula, where M is Cu(II) or Ni(II). For DAHK there are two such complexes, $MH_{-1}L$ and $MH_{-2}L$, differing by the protonation state of the lysine amine, which is not involved in coordination. For VIHN only the 4N species were detected, while potentiometric titrations indicated the presence of minor complexes MH_2L and ML for DAHKam. The actual existence of such complexes in XYH peptides is controversial [13,35], e.g. no CD signature could be found for them. As indicated by Fig. 2, these complexes, even if existing at low pH, are not present at pH 7.4, and therefore they were not taken under consideration for kinetic experiments.

Spectroscopic data presented in Table 3 (positions of CD spectral extrema for Cu(II) and Ni(II) complexes, and EPR parameters for Cu(II) species) indicate that 4N complexes of all three peptides are very similar to each other. In particular, the parameters for VIHN complexes do not deviate systematically from those of DAHam and DAHKam. This means that the side chain carboxylate of Asp1 does not have a direct effect on metal coordination (in agreement with previous observations [6,7]). A slight redshift of *d–d* bands accompanied by a subtle decrease of delocalization of the unpaired *d* electron of the Cu(II) ion in the DAHKam complex, compared to DAHam may be due to a tiny deviation from tetragonal symmetry caused by an interaction between the protonated Lys side chain and the His ring, observed previously in NMR studies of the Ni(II) complex of HSA [6].

Due to different protonation patterns, the stability constants of particular complexes of model peptides cannot be compared directly. There are two ways of circumventing this obstacle. One, allowing for comparisons of complexes with similar coordination modes and different protonation stoichiometries, uses the values of *K, the equilibrium constant of the actual complex formation reaction:

$$M + H_nL = MH_{-j}L + (n + j)H^+$$

This constant represents the overall ability of ligand L to form a given complex.

The other method is to calculate the conditional affinity constant at a given pH value, ^cK, corresponding to the following formal reaction, which ignores ligand protonation:

$$M + {^c}L = M{^c}L$$
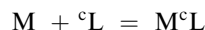
where ^cL is total ligand concentration. This constant is useful for comparing stabilities of metal complexes with dissimilar or not fully characterized ligands, such as proteins, for which the accurate protonation information is unavailable. Such comparisons are, however, limited to a particular pH value.

Both sets of constants are given in Table 6 for our model peptides and for related compounds. The cases of highest and lowest affinities were selected from literature data. The binding affinities for the model peptides are in the middle of the range of values for both Cu(II) and Ni(II). Note that the variation of side chain substituents can result in changes of complex stabilities by up to six orders of magnitude, without affecting the binding mode.

Kozlowski *et al.* have recently proposed to correlate the stabilities of 4N complexes of Xaa-Yaa-His peptides, expressed using *K constants, with the average basicities of the nitrogen donors of the peptide [37]. The constants measured in this work fall, however, below the correlation line proposed by them. This indicates that, while the basicities of nitrogen donors, partially dictated by side chains, is an important factor in complex stability, the outer sphere (steric) interactions also need to be considered.

Comparison of Cu(II) and Ni(II) binding between model peptides and albumins

Affinity for Ni(II) at site I can be compared between albumins on one hand and DAHam and DAHKam on the other. Much higher values were found for the complexes of model peptides. This fact was confirmed by an attempt to titrate DAHK-am with Ni(II) in 100 mM phosphate, analogously to albumins. The titration curve was linear,

Table 6. Logarithmic values of *K and ^cK constants for model peptides and other XYH peptide analogues, representing the high-end and the low-end of affinity series. The values of constants were calculated from appropriate stability constants, using formulae provided in the Materials and methods section.

Peptide	Log *K[a]		Log ^cK	
	Cu(II)	Ni(II)	Cu	Ni
VIHN[b]	−15.63	−19.75	13.0	8.8
DAHam[c]	−14.79	−20.02	13.7	8.5
DAHKam	−14.44	−19.48	13.8	8.7
GGH[d]	−16.43	−21.81	12.4	7.0
GGHist[e]	−17.14	−22.65	11.7	6.2
HmSHmSHam[f]	−11.05	−16.45	16.0	10.6
HP2$_{1-15}$ (RTHG-)[g]	−13.13	−19.29	14.5	8.5

[a] log *K = log $\beta(MH_{-j}L)$ − log $\beta(H_nL)$, j and n = 2, except for DAHKam, where j = 1 and n = 3. [b] Ni(II) data from ref [11]. [c] [31]. [d] [36].
[e] glycylglycylhistamine, [9]. [f] α-hydroxymetylseryl-α-hydroxymetylserylhistidinamide; Cu(II) data from [37]; Ni(II) data from [38].
[g] N-Terminal 15-peptide of human protamine 2, [35].

indicating that the Ni(II) was bound to DAHK-am so strongly that competition from phosphate was negligible. The ^cK values for Ni(II) complexes of HSA and BSA are still within the range provided by XYH peptides, but at its lower end (Tables 4 and 6). No direct measurements of Cu(II) affinities at site I have been reported so far, but estimates based on equilibrium dialysis and other indirect approaches, reviewed in [20], yield the log $^1K_{Cu}$ value of 12–13, confirming the trend found for Ni(II). We can only speculate on the reason of these differences, which might be due to different basicities of nitrogen donors at the protein surface, limited accessibility of the binding site due to shielding from the bulk of the protein, or some conformational interactions. The metal-free DAHK sequence in HSA has not been visualized in electron density maps, apparently due to its mobility in the crystals [1,22]. This does not necessarily exclude interactions of some kind between the site I complex and other parts of the protein in solution, which are in fact suggested by CD spectra (see below).

The comparison of CD spectra of complexes also points toward slight differences in the conformation of the chelate rings. The characteristic alternate pattern of the *d–d* bands in the CD spectra is dictated by the conformation of the six-membered chelate ring involving the His residue donors (Fig. 1). This conclusion is a direct consequence of the presence of the same kind of spectrum for 4N complexes of GGH, where the α carbon of the His residue is the sole source of chirality [10]. However, while positions of the component *d–d* bands and of CT transitions are relatively constant, their absolute and relative intensities depend quite strongly on the nonbonding substituents in positions 1, 2, and even 4 (Table 3). Moreover, the comparison with the spectra of albumin complexes clearly indicates the influence of the whole protein, which can only be transferred via the limitation of conformational freedom of the complex moiety. The CD spectra of HSA complexes are intermediate between those of DAHam and DAHKam, suggesting that the conformation of the chelate system in the protein is also intermediate between these two models.

The Cu(II) stabilities at site II were measured directly, by taking advantage from the presence of weakly competing phosphate ions. The Cu(II)/Ni(II) competition at site II was also studied. These experiments yielded binding values clearly lower from those obtained previously in the absence

of buffer [20]. The $^2K_{Cu}$ value decreased by ≈ 0.5 log units, while the K_r values increased by 1–1.5 log units (with K_r value for HSA still distinctly higher from that for BSA). This translates into a hundredfold decrease of Ni(II) affinity at site II in 100 mM phosphate buffer. It is possible that clustered histidines (His67 and His247, presumably providing metal binding at site II and the neighbouring His242) bind phosphate ions, thereby providing another level of competition for metal ion binding.

Kinetics of Ni(II) binding and Cu(II)/Ni(II) exchange

The data presented in Table 5 demonstrate that the process of Ni(II) binding has a uniform character for model peptides and for albumins. In all cases the apparent 1st order kinetics was found for this bimolecular reaction. The same reaction order was seen previously for the reverse reaction of acid decomposition of complexes, studied in detail for the Ni(II) complex of GGH [36,39]. The reason for this is the common slow step of the rearrangement of Ni(II) ion, between the high spin octahedral and the low spin square planar forms. The latter is present in the 4N complex, while the former in all other substrates/products in either case [13,40].

VIHN formed the most sluggish complex in both buffers, due to the additional step of side-chain folding [11]. The DAHKam complex exhibited the highest rate of formation in Tris, while DAHam reacted faster in phosphate. This suggests an assistant role of the Lys side chain in Ni(II) anchoring to DAHKam in Tris and its nonparticipation in phosphate, likely due to the blocking by phosphate ions, which would thereby compete with Ni(II). All the k_{obs} values for peptides were increased in the phosphate buffer. The increase was the most distinct for DAHam. The mechanism of catalysis of acid decomposition of nickel amine complexes by various compounds, including phosphates, was studied in detail [41]. In line with electrostatic considerations presented there, this rate enhancement is likely due to the facilitated anchoring of neutral NiHPO$_4$ to nitrogen donors of the peptide, compared to a positively charged Ni(II)–Tris complex.

The rates of Ni(II) complexation by albumins in phosphate are 10-fold lower from those for DAHam and DAHKam. This indicates that the metal-free DAHK

sequence in albumin is partially shielded from solution by the rest of the protein. There is no correlation between the complex stability and the rate of its formation.

The Ni(II) for Cu(II) exchange rates for peptides are of the order of 10^{-6} s^{-1} in Tris (again somewhat slower for VIHN, in accordance with the steric shielding of Ni(II)-N bonds [11,42]). These rates are markedly slower from that found for pure acid decomposition of the Ni(II)-GGH complex given in [39] ($k_d = 8 \times 10^{-5}$ s^{-1}). This, in conjunction with 1st order kinetics, suggests that the reaction of Ni(II) for Cu(II) exchange in Tris proceeds via Ni(II) complex dissociation (slow step), followed by the rapid formation of the Cu(II) species, and there is little assistance from the buffer components. There is no acceleration for DAHKam, compared to DAHam, in accordance with the lack of interaction between the Lys amine and Ni(II), once the 4N complex is formed.

The situation is quite different for phosphate solutions. The rate for DAHKam is now much lower from those of albumins, and the reaction of DAHam is much faster. The reaction rates for albumins and DAHam are higher from the value for pure acid GGH dissociation. The spread of rate constant values for the exchange reaction in phosphate is more than three orders of magnitude, compared to just one order for Ni(II) binding. These facts indicate that phosphate ions play a very specific role in Ni(II) dissociation and Cu(II) binding, different for each peptide. Note that the participation of phosphate is more likely to be of outer sphere character, because the presence of isodichroic points between the spectra of substrate (NiH$_j$L) and product (CuH$_j$L) in reaction mixtures points against a substantial formation of a ternary complex with mixed coordination by either metal ion.

The major difference between peptide and albumin experiments is in the form of existence of Cu(II). While it was present initially a weak phosphate complex in peptide experiments, it was bound at site II in quasi-steady state in albumin experiments (Fig. 5). This fact is confirmed by calculations of the occupancy of site II by Cu(II) and Ni(II) in the course of reaction, which yielded values of K_r for BSA identical to that obtained from direct titrations (log $K_r = 1.65 \pm 025$ vs. 1.63 ± 0.05, respectively).

Despite this fact, the values of k_{obs} for HSA and BSA, very similar to each other, are intermediate between those for DAHam and DAHKam. This shows that the mechanism of metal binding at site I in albumin cannot be modelled reliably by short peptides. The relatively fast rate of exchange of Ni(II) for Cu(II) suggests the presence of intramolecular Cu(II) transfer phenomenon in albumin. It seems that an unstructured (metal-free) site I cannot react according to this putative mechanism, because the Ni(II) binding reaction [which was in fact Ni(II) transfer from the kinetically labile site II to site I] was tenfold slower for the albumins than for both DAHam and DAHKam (Table 5). The possibility of an intermolecular interaction was excluded by the experiment in which the target molecule was the external DAHKam Ni(II) complex, with site I of HSA saturated with Cu(II). The rate constant measured in this experiment was identical, within the experimental error, with that obtained in the absence of albumin, and five times lower from that obtained with HSA alone. The similarity of rates between HSA and BSA suggests that this process may be common for albumins possessing site I. However, a rather vague theory that the spectroscopic and kinetic (but not even thermodynamic) properties of site I in HSA are equally well (poorly) modelled by DAHam and DAHKam peptides is as much as can be inferred from studies using peptide models for site I.

CONCLUSIONS

Our study demonstrated that the N-terminal site in HSA is much more similar to that of BSA than to short peptides reproducing the HSA sequence. The albumins bind Cu(II) and Ni(II) distinctly weaker than the model peptides. A very strong influence of phosphate ions on Cu(II) and Ni(II) binding at site II, as well as on kinetics of Ni(II) binding and substitution by Cu(II) at site I was found, but no structure–activity relationships between the binding sequence and reaction rate could be established. Our results clearly demonstrate that short peptides cannot be reliably used for interpretation and modelling of Cu(II) and Ni(II) transport by albumins. On the other hand, the direct thermodynamic and kinetic characterization of Ni(II) binding at site I in HSA and BSA was obtained. These data can be very useful in further studies of the toxicologically relevant Ni(II)-albumin complex. It would be also interesting to follow the indirect effects of physiologically relevant Ca^{2+} binding (which occurs at separate sites in the protein [20,21]) on metal ion binding at site II.

REFERENCES

1. Carter, D.C. & Ho, J.X. (1994) Structure of serum albumin. *Adv. Protein. Chem.* **45**, 153–203.
2. He, X.-M. & Carter, D.C. (1992) Atomic structure and chemistry of human serum albumin. *Nature* **358**, 209–214.
3. Peters,T. Jr (1985) Serum albumin. *Prot. Chem.* **37**, 161–245.
4. Glennon, J.D. & Sarkar, B. (1982) Nickel (II) transport in human blood serum. *Biochem. J.* **203**, 15–23.
5. Laussac, J.P. & Sarkar, B. (1984) Characterization of the copper (II) and nickel (II)-transport site of human serum albumin. Studies of copper (II) and nickel (II) binding to peptide 1–24 of human serum albumin by ^{13}C and ^{1}H NMR spectroscopy. *Biochemistry* **23**, 2832–2838.
6. Sadler, P.J., Tucker, A. & Viles, J.H. (1994) Involvement of a lysine residue in the N-terminus Ni^{2+} and Cu^{2+} binding site of serum albumins. Comparison with Co^{2+}, Cd^{2+}, Al^{3+}. *Eur. J. Biochem.* **220**, 193–200.
7. Valko, M., Morris, H., Mazúr, M., Telser, J., McInnes, E.J.L. & Mabbs, F.E. (1999) High-affinity binding site for copper (II) in human and dog serum albumins (an EPR study). *J. Phys. Chem. B* **103**, 5591–5597.
8. Camerman, N., Camerman, A. & Sarkar, B. (1976) Molecular design to mimic the copper (II) transport site of human albumin. The crystal and molecular structure of copper(II)-glycylglycyl-L-histidine-N-methyl amide monoaqua complex. *Can. J. Chem.* **54**, 1309–1316.
9. Gajda, T., Henry, B., Aubry, A. & Delpuech, J.-J. (1996) Proton and metal ion interactions with glycylglycylhistamine, a serum albumin mimicking pseudopeptide. *Inorg. Chem.* **35**, 586–593.

10. Bal, W., Djuran, M.I., Margerum, D.W., Gray, E.T. Jr, Mazid, M.A., Tom, R.T., Nieboer, E. & Sadler, P.J. (1994) Dioxygen-induced decarboxylation and hydroxylation of [Ni^{II}(glycyl-glycyl-L-histidine)] occurs via Ni^{III}: X-ray crystal structure of [Ni^{II}(glycyl-glycyl-α-hydroxy-D,L-histamine)]3H$_2$O. *J. Chem. Soc., Chem. Comm.* 1889–1890.

11. Bal, W., Chmurny, G.N., Hilton, B.D., Sadler, P.J. & Tucker, A. (1996) Axial hydrophobic fence in highly stable Ni(II) complex of des-angiotensinogen N-terminal peptide. *J. Am. Chem. Soc.* **118**, 4727–4728.

12. Bal, W., Wójcik, J., Maciejczyk, M., Grochowski, P. & Kasprzak, K.S. (2000) Induction of a secondary structure in the N-terminal pentadecapeptide of human protamine HP2 through Ni(II) coordination. An NMR study. *Chem. Res. Toxicol.* **13**, 823–830.

13. Kozlowski, H., Bal, W., Dyba, M. & Kowalik-Jankowska, T. (1999) Specific structure-stability relations in metallopeptides. *Coord. Chem. Rev.* **184**, 319–346.

14. Peters, T. Jr & Blumenstock, F.A. (1967) Copper-binding properties of bovine serum albumin and its amino-terminal peptide fragment. *J. Biol. Chem.* **242**, 1574–1578.

15. Appleton, D.W. & Sarkar, B. (1971) The absence of specific copper (II) -binding site in dog albumin. *J. Biol. Chem.* **246**, 5040–5046.

16. Callan, W.M. & Sunderman, F.W. Jr (1973) Species variations in binding of ^{63}Ni(II) by serum albumin. *Res. Comm. Chem. Pathol. Pharmacol.* **5**, 459–472.

17. Laurie, S.H. & Pratt, D.E. (1986) A spectroscopic study of nickel (II)–bovine serum albumin binding and reactivity. *J. Inorg. Biochem.* **28**, 431–439.

18. Rakhit, G. & Sarkar, B. (1981) Electron spin resonance study of the copper (II) complexes of human and dog serum albumins and some peptide analogs. *J. Inorg. Biochem.* **15**, 233–241.

19. Predki, P.F., Harford, C., Brar, P. & Sarkar, B. (1992) Further characterization of the N-terminus copper (II) and nickel (II) -binding motif of proteins. Studies of metal binding to chicken serum albumin and the native sequence peptide. *Biochem. J.* **287**, 211–215.

20. Bal, W., Christodoulou, J., Sadler, P.J. & Tucker, A. (1998) Multi-metal binding site of serum albumin. *J. Inorg. Biochem.* **70**, 33–39.

21. Sadler, P.J. & Viles, J.H. (1996) ^{1}H and ^{113}Cd NMR investigations of Cd^{2+} and Zn^{2+} binding sites on serum albumin: competition with Ca^{2+}, Ni^{2+}, Cu^{2+} and Zn^{2+}. *Inorg. Chem.* **35**, 4490–4496.

22. Sugio, S., Kashima, A., Mochizuki, S., Noda, M. & Kobayashi, K. (1999) Crystal structure of human serum albumin at 2.5 A resolution. *Protein Eng.* **12**, 439–446.

23. Dolovich, J., Evans, S.L. & Nieboer, E. (1984) Occupational asthma from nickel sensitivity. I. Human serum albumin in the antigenic determinant. *Br. J. Ind. Med.* **41**, 51–55.

24. Patel, S.U., Sadler, P.J., Tucker, A. & Viles, J.H. (1993) Direct detection of albumin in human blood plasma by ^{1}H NMR spectroscopy. Complexation of nickel (II). *J. Am. Chem. Soc.* **115**, 9285–9286.

25. Kasprzak, K.S., Jaruga, P., Zastawny, T.H., North, S.L., Riggs, C.W., Olinski, R. & Dizdaroglu, M. (1997) Oxidative DNA base damage and its repair in kidneys and livers of nickel (II) -treated male F344 rats. *Carcinogenesis* **18**, 271–277.

26. Meienhofer, J., Waki, M., Heimer, E.P., Lambros, T.J., Makofske, R.C. & Chang, C.D. (1979) Solid phase synthesis without repetitive hydrolysis. Preparation of leucylalanyl-glycyl-valine using 9-fluorenylmethyloxy- carbonylamino acids. *Int. J. Peptide Protein Res.* **13**, 35–42.

27. Fields, G.B., ed. (1997) Solid-Phase Peptide Synthesis. *Methods Enzymol.* 289. Academic Press, New York.

28. Chan, W.C. & White, P.D., eds. (2000) Fmoc Solid Phase Peptide Synthesis. *A Practical Approach.* Oxford University Press, New York.

29. Irving, H., Miles, M.G. & Pettit, L.D. (1967) A study of some problems in determining the stoichiometric proton dissociation constants of complexes by potentiometric titrations using a glass electrode. *Anal. Chim. Acta* **38**, 475–488.

30. Gans, P., Sabatini, A. & Vacca, A. (1985) SUPERQUAD: an improved general program for computation of formation constants from potentiometric data. *J. Chem. Soc. Dalton Trans.* 1195–1199.

31. Mlynarz, P., Valensin, D., Kociolek, K., Zabrocki, J., Olejnik, J. & Kozlowski, H. (2002) Impact of the peptide sequence on the coordination abilities of albumin-like tripeptides towards Cu^{2+}, Ni^{2+} and Zn^{2+} ions. Potential albumine-like peptide chelators. *New. J. Chem.* **26**, in press.

32. Chan, B., Dodsworth, N., Woodrow, J., Tucker, A. & Harris, R. (1995) Site-specific N-terminal auto-degradation of human serum albumin. *Eur. J. Biochem.* **227**, 524–528.

33. Banerjea, D., Kaden, T. & Sigel, H. (1981) Enhanced stability of ternary complexes in solution through the participation of heteroaromatic N bases. Comparison of the coordination tendency of pyridine, imidazole, ammonia, acetate, and hydrogen phosphate toward metal ion nitrilotriacetate complexes. *Inorg. Chem.* **20**, 2586–2590.

34. Fischer, B., Haring, U., Tribolet, R. & Sigel, H. (1979) Metal ion/buffer interactions. Stability of binary and ternary complexes containing 2-amino-2(hydroxymethyl)-1,3-propanediol (Tris) and adenosine 5′-triphosphate (ATP). *Eur. J. Biochem.* **94**, 523–530.

35. Bal, W., Jezowska-Bojczuk, M. & Kasprzak, K.S. (1997) Binding of nickel (II) and copper (II) to the N-terminal sequence of human protamine HP2. *Chem. Res. Toxicol.* **10**, 906–914.

36. Hay, R.W., Hassan, M.M. & Quan, C.Y. (1993) Kinetic and thermodynamic studies of the copper (II) and nickel (II) complexes of glycylglycyl-L-histidine. *J. Inorg. Biochem.* **52**, 17–25.

37. Mlynarz, P., Bal, W., Kowalik-Jankowska, T., Stasiak, M., Leplawy, M.T. & Kozlowski, H. (1999) Introduction of α-hydroxymethylserine residues in the peptide sequence results in the strongest peptidic copper (II) chelator known to date. *J. Chem. Soc. Dalton Trans.* 109–110.

38. Mlynarz, P., Gaggelli, N., Panek, J., Stasiak, M., Valensin, G., Kowalik-Jankowska, T., Leplawy, M.L., Latajka, Z. & Kozlowski, H. (2000) How the α-hydroxymethylserine residue stabilizes oligopeptide complexes with nickel (II) and copper (II) ions. J. Chem. Soc. Dalton Trans. 1033–1038.

39. Bannister, C.E., Raycheba, J.M.T. & Margerum, D.W. (1982) Kinetics of nickel (II) glycylglycyl-L-histidine reactions with acids and triethylamine. *Inorg. Chem.* **21**, 1106–1112.

40. Pettit, L.D., Pyburn, S., Bal, W., Kozlowski, H. & Bataille, M. (1990) A study of the comparative donor properties of the terminal amino and imidazole nitrogens in peptides. *J. Chem. Soc. Dalton Trans.* 3565–3570.

41. Read, R.A. & Margerum, D.W. (1982) Kinetics of hydrogen phosphate catalysed chelate ring opening in (ethylenediamine) nickel (II). *Inorg. Chem.* **22**, 3447–3451.

42. Raycheba, J.M.T. & Margerum, D.W. (1980) Effect of non-coordinative axial blocking on the stability and kinetic behavior of ternary 2,6-lutidine-nickel (II) -oligopeptide complex. *Inorg. Chem.* **19**, 837–843.